

Knocking-Down Cyclin A₂ by siRNA Suppresses Apoptosis and Switches Differentiation Pathways in K562 Cells upon Administration with Doxorubicin

Xiaohui Wang, Yujun Song, Jinsong Ren, Xiaogang Qu*

Division of Biological Inorganic Chemistry, State Key Laboratory of Rare Earth Resources Utilization, Changchun Institute of Applied Chemistry, Graduate School of the Chinese Academy of Sciences, Chinese Academy of Sciences, Changchun, Jilin, China

Abstract

Cyclin A₂ is critical for the initiation of DNA replication, transcription and cell cycle regulation. Cumulative evidences indicate that the deregulation of cyclin A₂ is tightly linked to the chromosomal instability, neoplastic transformation and tumor proliferation. Here we report that treatment of chronic myelogenous leukaemia K562 cells with doxorubicin results in an accumulation of cyclin A₂ and follows by induction of apoptotic cell death. To investigate the potential preclinical relevance, K562 cells were transiently transfected with the siRNA targeting cyclin A₂ by functionalized single wall carbon nanotubes. Knocking down the expression of cyclin A₂ in K562 cells suppressed doxorubicin-induced growth arrest and cell apoptosis. Upon administration with doxorubicin, K562 cells with reduced cyclin A₂ showed a significant decrease in erythroid differentiation, and a small fraction of cells were differentiated along megakaryocytic and monocyte-macrophage pathways. The results demonstrate the pro-apoptotic role of cyclin A₂ and suggest that cyclin A₂ is a key regulator of cell differentiation. To the best of our knowledge, this is the first report that knocking down expression of one gene switches differentiation pathways of human myeloid leukemia K562 cells.

Citation: Wang X, Song Y, Ren J, Qu X (2009) Knocking-Down Cyclin A₂ by siRNA Suppresses Apoptosis and Switches Differentiation Pathways in K562 Cells upon Administration with Doxorubicin. PLoS ONE 4(8): e6665. doi:10.1371/journal.pone.0006665

Editor: Hany A. El-Shemy, Cairo University, Egypt

Received: April 27, 2009; **Accepted:** July 7, 2009; **Published:** August 17, 2009

Copyright: © 2009 Wang et al. This is an open-access article distributed under the terms of the Creative Commons Attribution License, which permits unrestricted use, distribution, and reproduction in any medium, provided the original author and source are credited.

Funding: This work was supported by NSFC (20831003, 90813001, 20833006) and funds from the Chinese Academy of Sciences and Jilin Province. The funders had no role in study design, data collection and analysis, decision to publish, or preparation of the manuscript.

Competing Interests: The authors have declared that no competing interests exist.

* E-mail: xqu@ciac.jl.cn

Introduction

Tumor cells are characterized by deregulation of cell cycle checkpoints, leading to uncontrolled cell division and proliferation under conditions where non-transformed cells cannot enter and pass through the cell cycle. All these may come from over-expression of cyclins and the abnormal activation of cyclin-dependent kinases (CDKs) [1]. Cyclins are a superfamily of proteins whose levels vary in a cyclical fashion during the cell cycle to activate specific CDK required for the proper progression through the cell cycle. Cyclin A₂, which is essential for initiation and progression of DNA replication as well as for cell cycle progression through G1/S and G2/M transitions [2–5], is over-expressed in a variety of human cancers compared with normal cells and tissues [6–15]. Deregulated expression of cyclin A₂ seems to be closely associated with early events in tumor transformation [6,15]. In addition, its expression level in many types of cancers appears to be of prognostic value such as prediction of aggressiveness, survival or early relapse [9–14].

Until recently it has been held that CDK2, presumed master of the known CDK isoforms, is a promising anticancer target for developing small molecule inhibitors. The first-generation CDK inhibitors, flavopiridol and CY-202, are in late-stage clinical trials, and have only modest activity [16]. Recent findings [17], however, suggest that CDK2 may not be a key cell cycle player and question whether selective CDK2 inhibition is a useful cancer therapy

strategy. No cell cycle abnormalities are observed in either a CDK2 null mouse or following acute ablation of CDK2 in primary cells, indicating that this gene is not strictly required for cell proliferation [17]. In contrast, deletion of cyclin A₂ in knockout mice is associated with an embryonic lethal phenotype [18]. Moreover, Fine *et al.* demonstrated that cyclin A₂ and/or cyclin A₂-CDK2 complex but not CDK2 is a promising anticancer target with a high therapeutic index [19]. Therefore, inhibitors of CDK2 may not be appropriate for cancer therapy and more efforts are focused on inhibition of cyclin A₂ and/or cyclin A₂-CDK2 complex activity. We have shown that reduction of cyclin A₂ in human chronic myelogenous leukaemia K562 cells using small interfering RNA significantly inhibits cell proliferation [20], further supporting the notion that cyclin A₂ can serve as a novel therapeutic target.

Apoptosis and differentiation are the predominant two mechanisms by which chemotherapeutic agents kill tumor cells. Low dose of doxorubicin (DOX) induces erythroid differentiation in K562 cells, while high concentration of DOX promotes apoptosis [21]. Although many molecular pathways are involved in the apoptosis-regulatory mechanism, evidences suggest that the cell cycle and apoptosis may be interconnected [22–28]. Several studies have shown that increased expression of cyclin A₂ is found in cells in response to several apoptotic stimuli, but very few studies have dealt with this issue directly [29–33]. So it is important to clarify whether the decreased expression of cyclin A₂ is a cause of cell differentiation or a result of differentiation response.

Carbon nanotubes possess the unique features of being able to enter a living cell without causing its death or without inflicting other damage and can shuttle biological molecules into mammalian cells, indicating their potential application as a vector for the delivery of therapeutic molecules [34–36]. Recently we have reported that single wall carbon nanotubes (SWNTs) can induce a sequence-dependent B-A DNA transition [37], selectively induce human telomeric i-motif DNA formation [38], accelerate S1 nuclease cleavage rate [39], cause single-stranded poly(rA) to form a duplex structure and bind to human telomeric i-motif DNA under molecular-crowding conditions [40,41]. Herein, we explore whether altering the levels of cyclin A₂ in K562 cells using RNAi delivered by SWNTs can influence cell apoptosis and differentiation induced by chemotherapeutic agent DOX. K562 cells with reduced cyclin A₂ showed a significant decrease in growth suppression, apoptosis and erythroid differentiation, and were differentiated along megakaryocytic and macrophage-monocytic pathways upon administration with DOX. These findings indicate a positive correlation between cyclin A₂ and apoptosis induced by DOX and suggest that cyclin A₂ is a key regulator of cell differentiation, supporting the notion that cyclin A₂ is an important regulator for cell cycle as well as for cell apoptosis and differentiation. To the best of our knowledge, this is the first report that knocking down expression of one gene can switch K562 cells differentiation pathways.

Results

Upregulation of cyclin A₂ during apoptosis of K562 cells induced by DOX

DOX can inhibit growth of a variety of cancer cells [42]. To measure apoptosis rates induced by varying concentrations of DOX in K562 cells, we use acridine orange (AO)/ethidium bromide (EB) staining assay (Fig. 1). The percentage of apoptotic cells increased with time in a dose dependent fashion. RT-PCR and western blotting were used for studying the effect of DOX on the expression of cyclin A₂ in K562 cells. As shown in Fig. 2, cyclin A₂ expression levels increased with the increase of DOX, and a positive correlation was observed. These results show that expression of cyclin A₂ was significantly up-regulated in DOX-treated K562 cells at time points

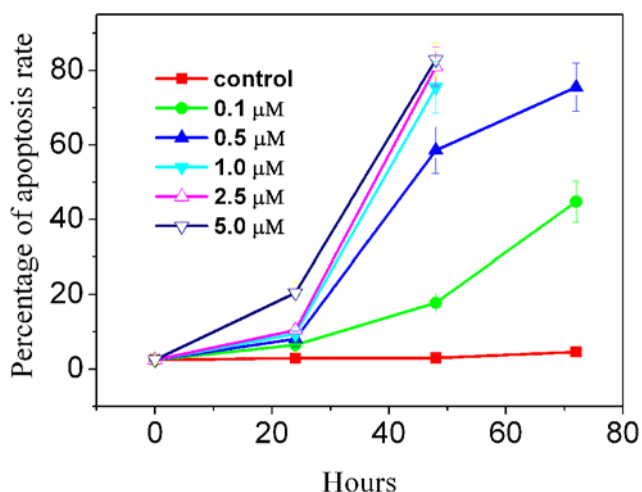


Figure 1. Dose- and time-dependent apoptosis of K562 cells upon administration with DOX. Apoptotic cells were determined by AO/EB staining. Tests were done in triplicate, counting a minimum of 300 total cells from at least three random microscope fields each. doi:10.1371/journal.pone.0006665.g001

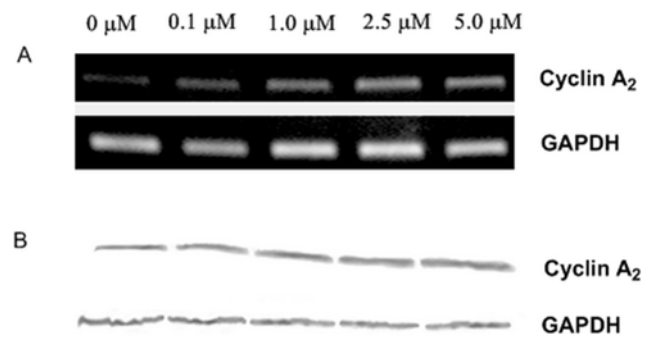


Figure 2. Expression of cyclin A₂ in K562 cells administered with varying concentrations of DOX. RT-PCR (A) and western blotting (B) were performed 32 hours and 60 hours after drug administration, respectively. doi:10.1371/journal.pone.0006665.g002

when DOX caused a significant amount of apoptosis, indicating that the levels of cyclin A₂ are correlated with the ability of DOX to induce apoptosis in K562 cells.

Suppression of DOX-induced growth inhibition by down-regulation of cyclin A₂ with siRNA delivered by SWNTs

We have previously demonstrated that functionalized single wall carbon nanotubes (SWNTs) can efficiently deliver siRNA targeting cyclin A₂ into K562 cells, resulting in specific suppression of cyclin A₂ expression [20]. Here, we use SWNTs to transfect cyclin A₂ siRNA into K562 cells and evaluate the effect of cyclin A₂ on growth inhibition induced by DOX. Two hours after transfection, DOX was added. Cell proliferation was examined by trypan blue exclusion method and methylthiazolyldiphenyl-tetrazolium bromide (MTT) assay. Fig. 3 showed cell growth curves of K562 cells after various treatments. It can be seen that depletion of cyclin A₂ inhibited cell proliferation while carbon nanotubes vector had no apparent effect on growth inhibition as well as no additive or synergetic effect on cell toxicology of DOX. DOX (0.4 μM) significantly suppressed cell growth, nevertheless, much less growth inhibition was observed in cells incubated with both cyclin

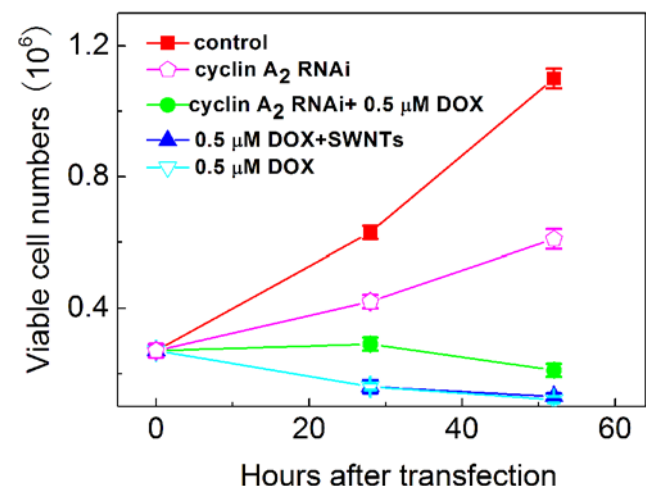


Figure 3. Growth curves of K562 cells in response to cyclin A₂ siRNA delivered by SWNTs and DOX. The viable cells were counted by trypan blue exclusion at indicated time points. The data shown here represent the average of two independent experiments. doi:10.1371/journal.pone.0006665.g003

A₂ siRNA and DOX, supported by microscopic results (Fig. S1). In order to further quantitatively investigate the effect of down-regulation of cyclin A₂ on the growth inhibition, MTT assays were carried out 24 h after incubation with DOX. Interaction of DOX with MTT was also checked in a cell free system and the results indicated that DOX showed no inference to MTT assay (Fig. S2). As shown in Fig. 4, IC₅₀ of non-transfected cells was about 2.5 μM. For siRNA transfected K562 cells, IC₅₀ was about 5.0 μM. The results clearly demonstrate that down-regulation of cellular cyclin A₂ level suppress DOX-induced growth inhibition.

Suppression of DOX-induced apoptotic cell death by down-regulation of cyclin A₂ with siRNA delivered by SWNTs

To investigate whether cyclin A₂ participates in cell apoptosis death and determine if reduction of cyclin A₂ has an effect on apoptosis induced by DOX, siRNA specific for cyclin A₂ was transfected into K562 cells by SWNTs, and low dose of DOX (0.4 μM) was administered. As shown in Fig. 5, carbon nanotubes vector showed no apparent cell toxicology, while numerous larger cells and typical lobular nuclei were observed in cells incubated with DOX. For cells coadministered with cyclin A₂ siRNA and DOX, much less apoptotic nuclei were observed, and the size of live cells was much bigger than that of the control cells. Statistics analysis showed that down-regulation of cyclin A₂ significantly reduced the apoptosis rate from more than 60% to about 20%. Similar results were obtained by annexin V-PI double staining flow cytometric technique (as shown in Figure S3). These clearly indicated lowering cyclin A₂ level in K562 cells led to suppression of apoptosis, thus a marked decrease in DOX susceptibility, which provide direct evidence that cyclin A₂ is involved in cellular responses to apoptosis.

The cytoplasmic subcellular distribution of cyclin A₂ correlates with apoptosis of K562 cells induced by DOX

Early reports have demonstrated that there is a link between cyclin A₂ subcellular localization and its cell function, and the level of cyclin A₂ is correlated to cell apoptosis [22,23,26]. For clarifying

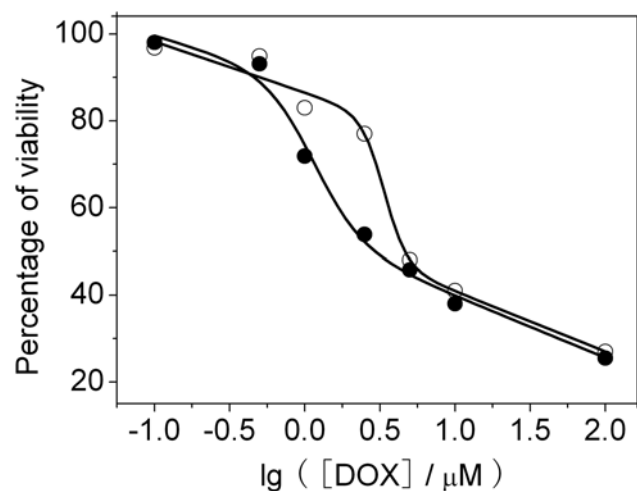


Figure 4. Effect of depletion of cyclin A₂ on the survival of K562 cells treated with DOX. Cells were transfected with cyclin A₂ siRNA (○) or not (●) two hours prior to the addition of drug. The viability was assessed by MTT assay as specified in Materials and Methods. The data shown here were means of two separate experiments performed in triplicate. doi:10.1371/journal.pone.0006665.g004

whether the subcellular distribution of cyclin A₂ in K562 cells correlates with apoptosis induced by DOX, indirect immunofluorescence detection of cyclin A₂ was performed. As shown in Fig. 6A, a significant fraction of cells underwent apoptosis and orange nuclei were observed, where DOX was mostly located. The immunofluorescence labeling of cyclin A₂ showed its presence predominantly in the nucleus of control K562 cells (Fig. S4), whereas in cells administered with DOX, cyclin A₂ was mainly located at the cytoplasm of early and late phases of apoptotic cells (Fig. 6B). Cyclin A₂ labeling was not found in the K562 cells incubated with non-immune serum (Fig. 6C). The results indicated that translocation of cyclin A₂ from the nucleus to cytoplasm was connected with its role in apoptosis.

Suppression of cyclin A₂ by siRNA can switch differentiation pathways of K562 cells induced by DOX

As mentioned above, cells treated with both cyclin A₂ siRNA and DOX were much bigger than the control. Since enlarged phenotype may suggest cell differentiation, we performed the benzidine staining to assess erythroid differentiation, which was the differentiation pathway of K562 cells upon treatment with anthracycline antibiotics including DOX [42,43]. Representative microscopy images of the benzidine staining in K562 cells after various treatments were shown in Fig. S5. For untreated cultures and cells administered with SWNTs, the percentages of benzidine positive cells were very low (less than 2%). Forty hours after incubation with DOX, around 14% benzidine positive cells were observed. However, down-regulation of cyclin A₂ by siRNA in K562 cells substantially suppressed erythroid differentiation upon administration with DOX (less than 1% benzidine positive cells, as shown in Fig. 7).

To determine whether K562 cells with reduced cyclin A₂ upon treatment with DOX underwent megakaryocytic pathway and monocyte-macrophage differentiation, which are the other two differentiation pathways of K562 cells, flow cytometric measurement of megakaryocytic specific surface antigen CD61 (GPIIIa) and nitro blue tetrazolium (NBT) reduction assay were carried out, respectively. As shown in Fig. S6, in comparison with the control, cells co-administered with cyclin A₂ siRNA and DOX showed significant increase in granularity measured by side scatter (side scatter, on *Y*-axis) and cell size measured by forward scatter (forward scatter, on *X*-axis), which was in good agreement with our AO/EB staining observation. Cells treated with DOX or SWNTs showed no detectable expression of CD61 (GPIIIa) (shown in Fig. S7), whereas in K562 cells co-administered with cyclin A₂ siRNA and DOX, the fraction of CD61 (GPIIIa) positive cells (~10%) was clearly observed (Fig. 8). For NBT reduction assay, representative microscopy images of K562 cells after various treatments were shown in Fig. S8. In cells treated with DOX or SWNTs, the percentage of NBT positive cells was very low (1%), whereas a small fraction NBT positive cells (~6%) was observed in K562 cells co-administered with cyclin A₂ siRNA and DOX (Fig. 9). Although the fractions of cells undergoing megakaryocytic pathway (~10%) and monocyte-macrophage differentiation (~6%) were small, the difference is statistically significant compared to the control group. Considering that DOX is an erythroid differentiation-inducing agent for K562 cells [21,42,43], it is not surprising that only a small fraction of K562 cells with reduced cyclin A₂ underwent megakaryocytic pathway and monocyte-macrophage differentiation.

Taken together, these results indicate that knocking down the expression of cyclin A₂ suppressed DOX-induced erythroid differentiation and a small fraction of K562 cells with reduced cyclin A₂ were differentiated along megakaryocytic and monocyte-

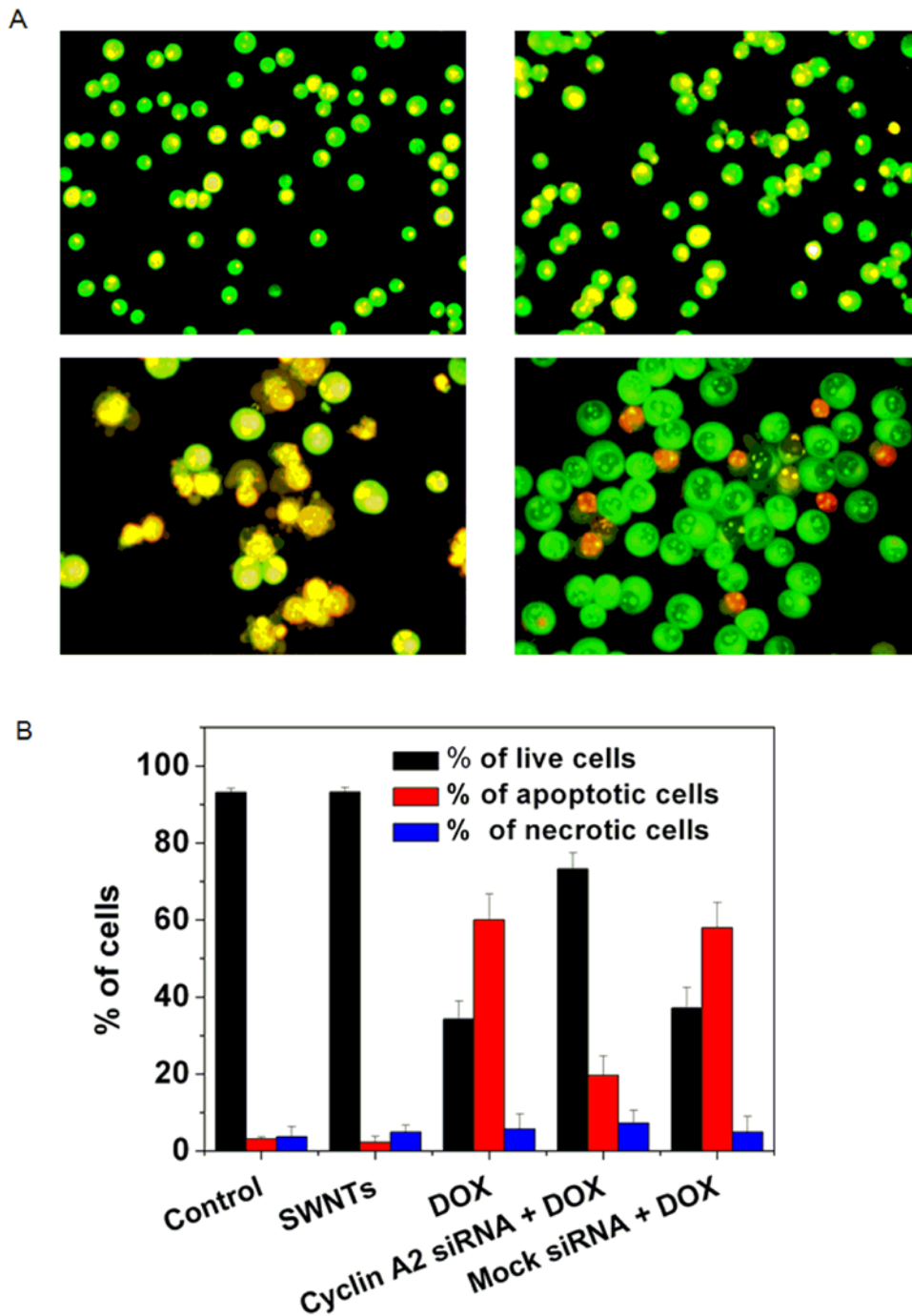


Figure 5. Morphological observation of K562 cells with a fluorescence microscope. Cells were stained with AO/EB dye mixture as described in Materials and Methods section. Shown here were the representative images of three separate experiments. (A): upper left, untreated control cells; upper right, cells treated with transfection vector SWNTs for 32 h; lower left, cells were incubated with 0.4 μ M DOX for 32 h, many cells appeared typical apoptotic bleb phenomenon; lower right, two hours after cyclin A₂ siRNA transfection, cells were then administered with 0.4 μ M DOX for additional 32 h. B: quantification of the live, apoptotic, and necrotic cells. Tests were done in triplicate, counting a minimum of 300 total cells each. doi:10.1371/journal.pone.0006665.g005

macrophage pathways upon treatment with DOX. These findings suggest that cyclin A₂ is an important regulator of cell differentiation.

Discussion

Cyclin A₂ is particularly interesting among the cyclin family because it can activate two different CDKs and functions in both S

phase and mitosis. In S phase, phosphorylated cyclin A₂-CDK2 complexes are suggested to play an important role in the initiation of DNA replication. In mitosis, cyclin A₂ may contribute to the control of cyclin B stability. Consistent with its role as a key cell cycle regulator, overexpression of cyclin A₂ is associated with transformed cells [6–15]. However, it is difficult to determine whether elevation of cyclin A₂ is a contributing factor or a mere

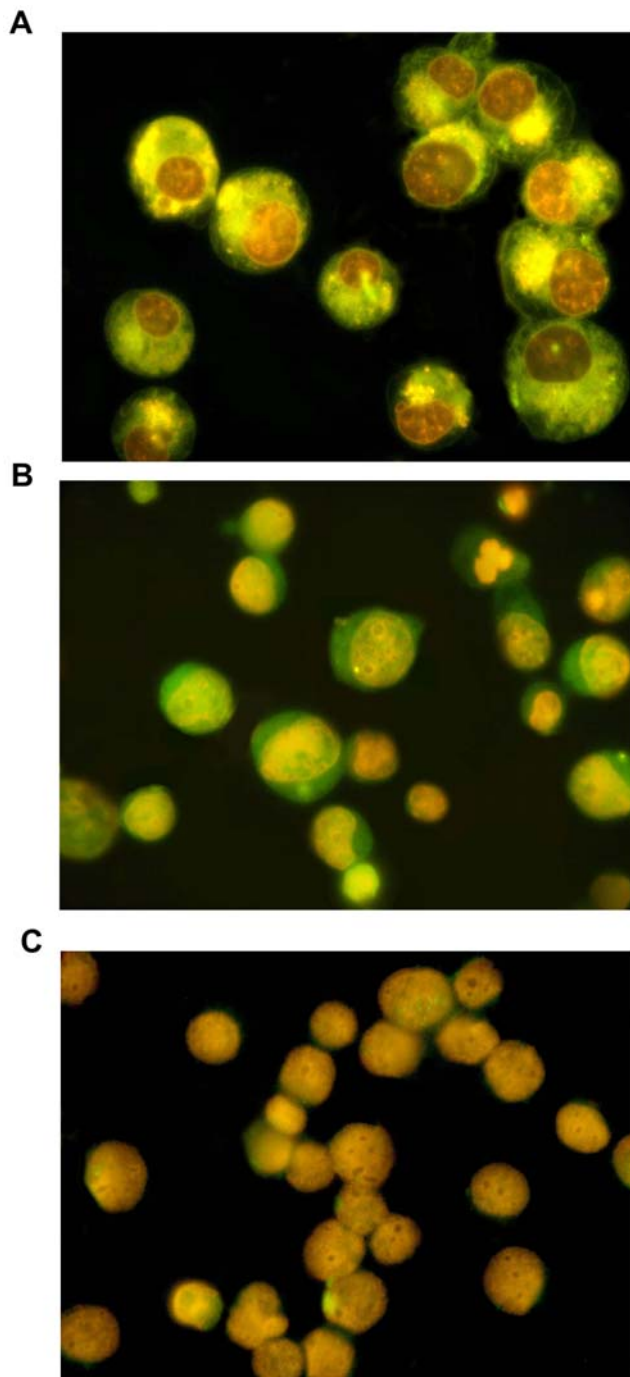


Figure 6. The sub-cellular distribution of cyclin A₂ in K562 cells correlated with cell apoptosis. Cells were administered with 0.4 μM DOX for 32 h. A significant fraction of cells underwent apoptosis. Immunofluorescence detection of cyclin A₂ was performed as described in Materials and Methods section. A: representative fluorescence microscopy image of K562 cells after treatment. Orange nuclei were observed, where DOX was mostly located; B: representative immunofluorescence microscopy image of K562 cells. Cyclin A₂, normally located at nucleus, can be observed in cytoplasm of early and late phases of apoptotic cells. C: representative microscopy image of negative control immunofluorescence in K562 cells. No significant non-specific signal was observed.

doi:10.1371/journal.pone.0006665.g006

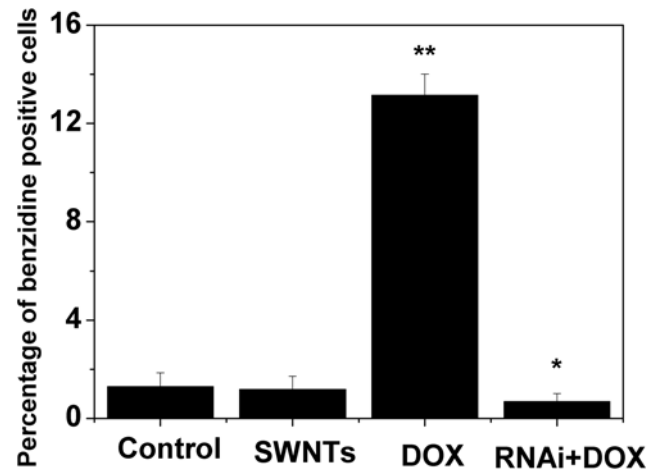


Figure 7. Knocking-down the expression of cyclin A₂ in K562 cells significantly inhibited erythroid differentiation induced by low concentration DOX. Cells were transfected with cyclin A₂ siRNA or not two hours prior to the addition of 0.4 μM DOX. Forty hours later, erythroid differentiation was scored by the benzidine staining method to determine the percentage of hemoglobin-positive K562 cells. Tests were done four times, counting a minimum of 300 total cells from at least three random microscope fields each. * $p < 0.05$, ** $p < 0.001$ vs. control untreated cells by Student's t-test. doi:10.1371/journal.pone.0006665.g007

consequence of the increased cell proliferation. In haematological malignancies, cyclin A₂ is associated with proliferation rate of these disorders and can be used for molecular diagnostics as a proliferation marker [13,14].

Single-walled carbon nanotubes (SWNTs) have been considered as the leading candidate for nanodevice applications ranging from gene therapy and novel drug delivery to membrane separations. We have previously showed that siRNA transfection efficiency of lipofectamine 2000 in K562 cells was low (28%) and some cells underwent apoptosis and necrosis during the process [20]. However, SWNTs could efficiently facilitate the coupling of siRNA to form siRNA:SWNTs complexes and carry siRNA into K562 cells, significantly knocking down the expression of target gene. No apparent cell toxicology was observed. Hence, in order to directly probe whether cyclin A₂ participates in cell apoptosis and differentiation, we employed SWNTs as transfection vector to deliver cyclin A₂ siRNA into K562 cells to specifically knock down the expression of cyclin A₂ and found that carbon nanotubes vector showed no additive or synergetic effect on cell toxicology of DOX, which was consistent with our previous report [20].

DOX, a prominent member of anthracycline antibiotics, has been extensively used for treatment of solid tumors and leukemia. It exerts its cytotoxic activity against cancer cells mainly by intercalation into DNA, inhibition of topoisomerase II and helicase activity, leading to cell-cycle arrest at the G₂/M phase and apoptosis [42]. In clinical applications, doses of DOX are strictly limited by its cardiotoxicity [43]. It should be noted that the dose of DOX administered here (0.4 μM) is pharmacological relevant compared to the initial or steady-state plasma concentrations observed in patients after standard bolus infusions (5 μM and 25–250 nM, respectively).

It has been reported that there is a link between cyclin A₂ and apoptosis [22–28]. Hoang *et al.* showed that in c-myc overexpressing serum deprived rat 1A fibroblasts undergoing apoptosis, cyclin A₂ mRNA expression was increased, in contrast to the invariant expression for cyclin B, C, D1 and E [24]. Moreover, serum-deprived rat 1A fibroblast stably transfected with cyclin A₂ exhibited

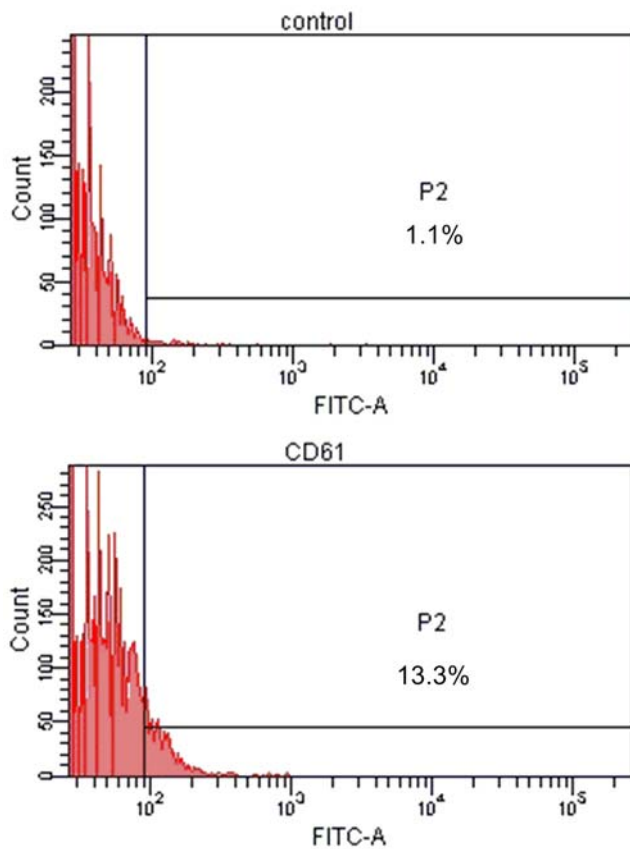


Figure 8. Flow cytometric measurement of megakaryocytic specific surface antigen CD61 (GPIIIa) in K562 cells co-administered with cyclin A₂ siRNA and DOX. Cells were transfected with siRNA by SWNTs two hours prior to the administration of 0.4 μ M DOX. Sixty hours later, expressions of CD61 (GPIIIa) were evaluated by using FITC-conjugated isotype control immunoglobulin and specific anti-CD61 (GPIIIa) FITC-conjugated monoclonal antibody. The marker placed to the right of histogram designates positive events. doi:10.1371/journal.pone.0006665.g008

increased apoptosis following stimulation of cyclin A₂ expression. Meikrantz *et al.* reported that induction of apoptosis was uniformly associated with activation of cyclin A₂-dependent kinases but not associated with cyclins E or B, and overexpression of the cyclin A₂ could circumvent the anti-apoptosis activity of the oncogene BCL-2 in human HeLa cells [25,26]. Furthermore, Hiromura *et al.* indicated that apoptosis was associated with an increase in cytoplasmic cyclin A₂-CDK2 activity following UV irradiation, under these conditions, nuclear cyclin A₂-Cdk2 activity decreased significantly [27]. Our results showed knocking down the expression of cyclin A₂ in K562 cells significantly suppressed the apoptosis induced by DOX and a positive correlation between the levels of cyclin A₂ and apoptosis was observed. The findings also indicate that the cytoplasmic subcellular distribution of cyclin A₂ correlates with its pro-apoptotic role. We speculate that cyclin A₂ associated kinases are involved in DOX-induced apoptotic cell death pathways in K562 cells, although the exact downstream mechanisms are not known.

We have demonstrated that SWNTs could effectively deliver cyclin A₂ siRNA into K562 cells, significantly suppressing the expression of cyclin A₂ with specificity and cell proliferation, and cells with reduced cyclin A₂ showed a decrease in the percentage of cells in S phase [20]. Several studies have indicated that cancer cells with a high S-phase fraction/high proliferative activity are more sensitive to apoptosis induced by chemotherapy [44,45]. As

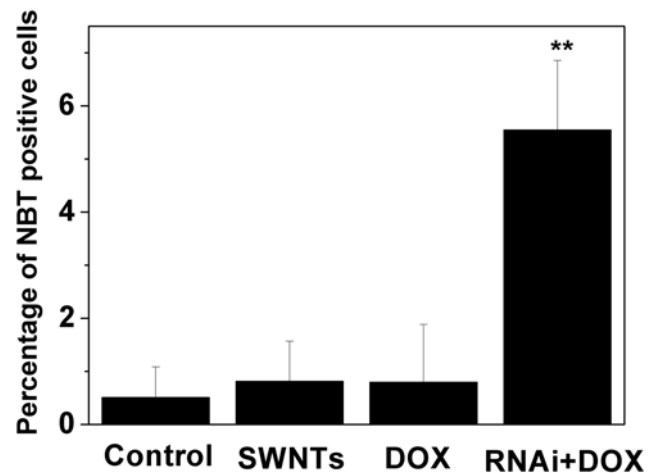


Figure 9. Knocking-down expression of cyclin A₂ in K562 cells induced monocyte-macrophage differentiation upon administration of DOX. Cells were transfected with siRNA by SWNTs two hours prior to the treatment of 0.4 μ M DOX. Ninety six hours later, NBT dye reduction was used to qualitatively monitor monocyte-macrophage differentiation. Tests were done twice, counting a minimum of 300 total cells from at least three random microscope fields each. ** p <0.001 vs. control untreated cells by Student's t-test. doi:10.1371/journal.pone.0006665.g009

for DOX, it is active throughout the cell cycle, but the effect is most pronounced for cells in S phase-G2 phase, especially in S phase, where it interferes with the DNA replication and transcription [42]. Therefore, it was not surprising that K562 cells with reduced cyclin A₂ showed a marked decrease in DOX susceptibility.

Most of chemotherapeutic agents show significant side effects and not all patients benefit from aggressive chemotherapy. Therefore, searching for tumor biological factors which can predict patient prognosis and chemotherapy response would be of most importance. Several studies have indicated that a high level of cyclin A₂ expression may be a marker of poor prognosis in cancers [10–13]. Besides, previous studies have shown that cancer patients with high level of cyclin A₂ had better chemotherapy response and survival than those with reduced cyclin A₂ and low expression of cyclin A₂, indicating that the patients with high expression of cyclin A₂ are more suitable for chemotherapy [46–48]. Our results demonstrate the pro-apoptotic role of cyclin A₂ in human myeloid leukemia K562 cells, and indicate that cells with low level of cyclin A₂ were more resistant to chemotherapeutic agent DOX. Poon *et al.* have suggested that a decrease of cyclin A₂, rather than increase, promotes tumorigenesis, and once the tumor has developed, high levels of cyclin A₂ simply reflect a high proliferation rate, which can explain this inconsistency [49]. Hence, despite its association with transformed cells, evaluating cyclin A₂ level in patients will be an important prognostic marker for use of chemotherapy. Patients with high level of cyclin A₂ may be more responsive to anticancer drugs through the induction of apoptotic cell death. Moreover, it should be cautious to combine doxorubicin chemotherapy with any small molecule drug targeting cyclin A₂/cyclin A₂ associated kinases since it can enhance potential drug resistance.

In several systems, it has been reported that down-regulation of cyclin A₂ and its associated CDK 2 activity are important for successful differentiation [29–33]. Ito *et al.* have suggested cyclin A₂ overexpression is directly related with poor differentiation [31]. Kiyokawa *et al.* have indicated that differentiation of murine

erythroleukemia cells induced by hexamethylene is accompanied by a decrease in the level of cyclin A₂ and CDK2 proteins and the persistent suppression of cyclin A₂ expression may play a role in HMBA-induced commitment to terminal differentiation [30]. Yoshizumi *et al.* showed down-regulation of cyclin A₂ gene expression *in vivo* at both the RNA and protein levels appears to be important in the permanent withdrawal of human and rat cardiomyocytes from the cell cycle during development [32]. Moreover, Rieber *et al.* demonstrated that the interaction of cyclin A₂ with E2F is the target for tyrosine induction of B16 melanoma terminal differentiation [33]. In this work, we found that knocking down the expression of cyclin A₂ in K562 cells significantly suppressed DOX-induced erythroid differentiation and a small fraction of cells with reduced cyclin A₂ were differentiated along megakaryocytic and monocyte-macrophage pathways upon treatment with DOX. To the best of our knowledge, this is the first report that knocking down expression of one gene can switch K562 cells differentiation pathways. The results suggested that cyclin A₂ is directly involved in the checkpoint of cell differentiation pathways and is a key regulator of this process, although the detail downstream mechanisms are not known. For cancer cells with low level of cyclin A₂, which are less responsive to chemotherapeutic agents, induction of differentiation might be an alternative strategy. Combination of cyclin A₂ siRNA and DOX may provide a novel option of such therapeutic strategy.

In conclusion, knocking down the expression of cyclin A₂ by siRNA delivered by SWNTs suppresses apoptosis and erythroid differentiation, and promotes megakaryocytic and monocyte-macrophage differentiation in human chronic myelogenous leukaemia K562 cells upon administration with DOX. The results demonstrate the pro-apoptotic role of cyclin A₂ and suggest that cyclin A₂ is a key regulator of cell differentiation, supporting the notion that cyclin A₂ is an important regulator for cell cycle as well as for cell apoptosis and differentiation.

Materials and Methods

Ethics statement. The human erythroleukemic cell line K562 [20] was used in this study.

Chemicals

Doxorubicin (DOX), Acridine Orange (AO), Ethidium Bromide (EB), Methylthiazolyl-diphenyl-tetrazolium bromide (MTT), DAPI, Nitro blue tetrazolium (NBT), benzidine and SWNTs ($\phi = 1.1$ nm, purity >90%) were purchased from Sigma-Adrich (St. Louis, MO, USA). Annexin V apoptosis detection kit was obtained from Keygentec (Nanjing, China). The dye mix for the EB/AO staining was 100 $\mu\text{g}/\text{mL}$ acridine orange and 100 $\mu\text{g}/\text{mL}$ ethidium bromide in phosphate buffered saline (PBS).

Cell culture

The human erythroleukemic cell line K562 [20] was grown in Iscove's modified Dulbecco's medium (Gibco BRL) supplemented with 10% fetal calf serum in a humidified 37°C incubator with 5% CO₂. Cells were passed three times per week. DNA fluorochrome staining (DAPI or Hoechst 33258) is used as our routine mycoplasma detection and the cells used for experiments are free of contamination. Exponentially growing cells were used for all experiments described below. Cell viability was determined by trypan blue exclusion in a haemocytometer chamber.

Transfection

The siRNA oligonucleotides were synthesized by Genepharma Corporation (Shanghai, China). The sequence used for targeting

silencing of cyclin A₂ was 5'-CCAUUGGUC CCUCUU-GAUUTT-3'. The nonsilencing control siRNA is an irrelevant siRNA with random nucleotides UUCUCCGAACGUGUCAC-GUTT. Functionalized single wall nanotubes (f-SWNTs) were prepared according to method described in our previous work [20]. Cyclin A₂ siRNA: f-SWNTs complexes ($w_{\text{f-SWNTs}}/w_{\text{siRNA}} = 40$) were added at 25 n mol/L (siRNA concentration) to culture of cells.

Reverse transcriptase-polymerase chain reaction (RT-PCR)

Total RNA was extracted using Trizol reagent (Invitrogen) according to the manufacturer's instructions. The primers and conditions for cyclin A₂ were TCCATGTCAGTGCCTGAGAGGA (5'), GAAGGTCCATGAGACAAGGC (3'); 94°C for 30 seconds, 60°C for 30 seconds, 72°C for 1 minute for 25 cycles. Three introns are present in this pair of primer so that any contaminating genomic DNA would not be amplified. Primers used for the glyceraldehyde-3-phosphate dehydrogenase (GAPDH) were ACCTGACCTGCCGTCTAGAA (5'), TCCACCACCCTGTTGCTGTA (3'). Two sets of primers were used for each sample, including primers specific for the gene of cyclin A₂ and primers for GAPDH as an internal control. All PCR products were visualized on 1.5% agarose gel with 0.5 $\mu\text{g mL}^{-1}$ EB.

Western blotting

For Western blot analysis, cells were lysed in radio-immunoprecipitation assay (RIPA) buffer (150 mmol/L NaCl, 50 mmol/L Tris-HCl, 0.5% sodium deoxycholate, 1% NP-40, 0.1% SDS, pH 7.6) containing protease inhibitors for protein extraction. Protein concentrations were determined using the Bradford assay. 20 μg cell samples were denatured by addition of 2 \times reducing sample buffer (100 mmol/L Tris, 4% SDS, 25% glycerol, 10% β -mercaptoethanol, 0.01% bromophenol blue, pH 6.8), incubated for 10 minutes at 95°C, and separated on a 12% SDS-PAGE. The proteins were electroblotted to PVDF membrane. After blocking with Tris-buffered saline containing 0.05% Tween 20 (TTBS) and 2% BSA, the membranes were incubated overnight at 4°C with appropriate primary antibody diluted in TTBS. Working dilutions were: 1/500 rabbit polyclonal anti-cyclin A₂ primary antibody (Lab Vision Corporation, CA, USA); 1/400 anti-GAPDH primary antibody (Santa Cruz, CA, USA). The membranes were washed three times in TTBS for 5 min each and then incubated for 1 h at room temperature with goat anti-rabbit IgG conjugated to horseradish peroxidase (Jackson ImmunoResearch, Stratech, UK). After extensive washing in TTBS, the protein-antibody complexes were visualized by CN/DAB substrate according to method described by Yong [50]. Images were photographed using a UVP gel documentation system (Ultraviolet Products, Upland, CA, USA).

MTT assay

K562 cells were plated in 96-well culture plate at a concentration of 0.5×10^4 cells/well, and were transfected with cyclin A₂ siRNA or not by SWNTs. Two hours later, the cells were treated with various concentrations of DOX while the blank control wells were added medium without drug. Cells were then cultured for another 24 hours and 20 μL MTT (5 mg/mL) was added in each well, followed by additional four hour incubation. The supernatants were then discarded carefully and 150 μL dimethylsulphoxide was added and shaken vigorously to dissolve the purple precipitation formation. Optical density (OD) of each well was tested using Bio-Rad model-680 microplate reader with a wavelength of 490 nm.

Cell fluorescence staining

Cells were collected by centrifugation at $200\times g$ for 5 minutes, and then washed twice with PBS. Cell concentration was adjusted as 2×10^6 – 5×10^6 cells/mL. 1 μ L EB/AO dye mix was added in 10 μ L cell suspension, followed by 10 minutes of incubation in dark. Stained cells suspension were placed on a clean microscope slide and covered with a cover-slip. Cells were viewed and counted using an Olympus BX-51 optical system microscope (Tokyo, Japan) at $400\times$ magnification with a blue filter. Pictures were taken with an Olympus digital camera. We note that the definition is sharper by eye through the microscope than in the photo. Tests were done in triplicate, counting a minimum of 300 total cells from at least three random microscope fields each.

Indirect immunofluorescence detection

Cells were harvested, washed three times with PBS, fixed with 4% paraformaldehyde in PBS for 30 min at 4°C and permeabilized with 0.5% Triton X-100 in PBS for 5 min at 4°C. After blocking in 10% goat serum, primary cyclin A₂ antibody (rabbit, polyclonal; Lab Vision Corporation, CA) was diluted to 1:400. Goat anti-rabbit FITC-conjugated secondary antibody (Jackson ImmunoResearch, Stratech, UK) was used at a 1:200 dilution. If necessary, DAPI was used to visualize cell nuclei. Cells were observed and photographed by fluorescence microscopy with oil immersion objective and appropriate filters.

Benzidine Staining

Erythroid differentiation was scored by the benzidine staining method for the determination of the percentage of hemoglobin-positive K562 cells induced by low concentration DOX. Briefly, cells were washed twice and then resuspended in 20 μ L PBS. 10 μ L of benzidine solution (0.2% benzidine, 0.6% H₂O₂, 0.5 M acetic acid) was added and incubated for 20 min at room temperature in the dark. Benzidine-positive cells (blue-black staining) were quantitated by light microscopy. At least 300 cells were counted in triplicate for each condition.

Flow cytometry analysis

Expression of GPIIIa is considered the most selective marker of the megakaryocyte lineage since it is not expressed on cells of other hematopoietic lineages from normal human bone marrow. Hence, staining of cells for surface CD61 (GPIIIa) was used to evaluate megakaryocytic differentiation. It employed a mouse monoclonal antibody fluorescein isothiocyanate (FITC)-conjugated anti-CD61 (eBioscience) or isotype-matched immunoglobulin (IgG1-FITC, eBioscience) at a concentration of 0.6 μ g/mL. Cells were harvested, washed, resuspended in PBS containing 10% fetus calf serum and 0.1% NaN₃ and incubated for 30 min on ice with antibodies in the dark. After washing three times, cells were resuspended in PBS containing 0.5% formaldehyde and 0.1% NaN₃, and then analyzed on a FACS Arial cytometer (Becton-Dickinson, San Diego, CA, USA). Viable cells were gated using forward and side scatter characteristics. Fluorescence intensity data were acquired using the BD FACSDIVA™ software.

NBT reduction assay

NBT dye reduction was used to qualitatively monitor monocyte-macrophage differentiation. Briefly, cells were collected, washed with PBS and resuspended in IMDM medium without serum. Cells suspension were mixed with an equal volume of 0.1% NBT dissolved in PBS and incubated at 37°C for 40 min. NBT was reduced to insoluble formazan because of the intracellular oxygen radical release in the cells differentiated to monocytes-macro-

phages. The percentage of cells containing intracellular reduced blue-black formazan was determined by light microscopy. At least 300 cells per preparation were observed.

Statistical analysis

Data are expressed as mean \pm s.d. and analysis of variance was carried out using Student's t test with Origin 7.5 (OriginLab Corporation, Northampton, MA, USA), where $p < 0.05$ was considered significant.

Supporting Information

Figure S1 Knocking-down the expression of cyclin A2 in K562 cells significantly suppressed growth inhibition and apoptosis induced by DOX. Cells were plated in 6-well plate at a density of 0.8×10^5 cells/mL and transfected with cyclin A2 siRNA (A, B) or not (C, D) by SWNTs two hours prior to the administration of 0.4 μ M DOX. 96 hours later, cells were viewed using an inverted microscope with objectives $\times 10$ (A, C) and $\times 40$ (B, D). Pictures were taken with an Olympus digital camera. Shown here are the representative images of three independent experiments. Found at: doi:10.1371/journal.pone.0006665.s001 (0.72 MB TIF)

Figure S2 Chemical interaction of DOX with MTT assay. The assay was performed as follows: 200 μ L of medium containing DOX at different concentrations was placed in a 96-well plate; 20 μ L of MTT solution (5 mg/mL) was added to each well; After incubation for 4 h at 37°C, 150 μ L of DMSO was added to each well and absorbance at 490 nm was measured in a Bio-Rad model-680 microplate reader. DOX-free complete medium was used as control and was treated in the same way as the DOX-containing media. Variation (%) = (absorbance of DOX containing medium - absorbance of control)/absorbance of control $\times 100$. Found at: doi:10.1371/journal.pone.0006665.s002 (3.08 MB TIF)

Figure S3 Annexin V-PI double staining of cells after various treatments. Upper left, untreated control; upper right, cells treated with transfection vector SWNTs; lower left, cells treated with 0.4 μ M DOX for 32 h; lower right, two hours after cyclin A2 siRNA transfection, cells were then administered with 0.4 μ M DOX for additional 32 h. Found at: doi:10.1371/journal.pone.0006665.s003 (0.24 MB TIF)

Figure S4 Indirect immunofluorescence detection of cyclin A2 in control K562 cells. DAPI was used to visualize cell nuclei. Cells were viewed using an Olympus BX-51 optical system microscope (Tokyo, Japan) with oil lens and appropriate filters. Representative stained fields are shown: (A), DAPI staining (blue); (B), immunofluorescence detection of cyclin A2 (FITC, green); (C) merged image. As indicated, cyclin A2 was located at the nucleus of K562 cells without DOX treatment. Found at: doi:10.1371/journal.pone.0006665.s004 (0.43 MB TIF)

Figure S5 Representative microscopy images of the benzidine staining of K562 cells after various treatments. Cells were transfected with cyclin A2 siRNA or not two hours prior to the addition of 0.4 μ M DOX. Forty hours later, erythroid differentiation was scored by the benzidine staining method as described in Materials and Methods section. Cells were viewed and counted using an Olympus BX-51 optical system microscope (Tokyo, Japan) at $200\times$ magnification. Four independent tests were performed. Pictures were taken with an Olympus digital camera. Found at: doi:10.1371/journal.pone.0006665.s005 (0.65 MB TIF)

Figure S6 Morphological changes of K562 cells after various treatments. Cells were transfected with cyclin A2 siRNA or not two hours prior to the administration of 0.4 μ M DOX. Cells were

then cultured for another 32 hours. Flow cytometry was used to show changes in size (forward scatter, on X-axis) and granularity (side scatter, on Y-axis). No significant morphological changes of K562 cells were observed upon RNAi mediated by SWNTs compared to the control. Cells administered with DOX underwent G2/M arrest and changes in granularity and cell size were clearly observed. Although knocking-down the expression of cyclin A2 by RNAi significantly inhibited growth suppression and apoptosis induced by DOX, cells co-administered with siRNA targeting for cyclin A2 and DOX showed similar increases in cell size and granularity compared to those treated with DOX alone.
Found at: doi:10.1371/journal.pone.0006665.s006 (2.11 MB TIF)

Figure S7 Flow cytometric measurement of megakaryocytic specific surface antigen CD61 (GPIIIa) in K562 cells. Cells were incubated with 0.4 μM DOX (A, B) or SWNTs (C, D) for 60 h. Expressions of CD61 (GPIIIa) were evaluated by using FITC-conjugated isotype control immunoglobulin (A, C) and specific anti-CD61 (GPIIIa) FITC-conjugated monoclonal antibody (B, D). The marker placed to the right of histogram designates positive events. K562 cells administrated with low concentration of DOX or SWNTs did not undergo apparent megakaryocytic differentiation.

References

- Hartwell LH, Kastan MB (1994) Cell cycle control and cancer. *Science* 266: 1821–1828.
- Lehner CF, O'Farrell PH (1989) Expression and function of *Drosophila* cyclin A during embryonic cell cycle progression. *Cell* 56: 957–968.
- Girard F, Strausfeld U, Fernandez A, Lamb NJ (1991) Cyclin A is required for the onset of DNA replication in mammalian fibroblasts. *Cell* 67: 1169–1179.
- Pagano M, Pepperkok R, Verde F, Ansorge W, Draetta G (1992) Cyclin A is required at two points in the human cell cycle. *EMBO J* 11: 961–971.
- Sobczak-Thopot J, Harper F, Florentin Y, Zindy F, Brecht C, et al. (1993) Localization of cyclin A at the sites of cellular DNA replication. *Exp Cell Res* 206: 43–48.
- Bui KC, Wu F, Buckley S, Wu L, Williams R, et al. (1993) Cyclin A expression in normal and transformed alveolar epithelial cells. *Am J Respir Cell Mol Biol* 9: 115–125.
- Huhtanen RL, Blomqvist CP, Böhling TO, Wiklund TA, Tukiainen EJ, et al. (1999) Expression of cyclin A in soft tissue sarcomas correlates with tumor aggressiveness. *Cancer Res* 59: 2885–2890.
- Li JQ, Miki H, Wu F, Saoo K, Nishioka M, et al. (2002) Cyclin A correlates with carcinogenesis and metastasis, and p27(kip1) correlates with lymphatic invasion, in colorectal neoplasms. *Hum Pathol* 33: 1006–1015.
- Volm M, Koomägi R, Mattern J, Stammers G (1997) Cyclin A is associated with an unfavourable outcome in patients with non-small-cell lung carcinomas. *Br J Cancer* 75: 1774–1778.
- Chao Y, Shih YL, Chiu JH, Chau GY, Lui WY, et al. (1998) Overexpression of cyclin A but not Skp 2 correlates with the tumor relapse of human hepatocellular carcinoma. *Cancer Res* 58: 985–990.
- Poikonen P, Sjostrom J, Amiri RM, Villman K, Ahlgren J, et al. (2005) Cyclin A as a marker for prognosis and chemotherapy response in advanced breast cancer. *Br J Cancer* 93: 515–519.
- Mrena J, Wiksten JP, Kokkola A, Nordling S, Haglund C, et al. (2006) Prognostic significance of cyclin A in gastric cancer. *Int J Cancer* 119: 1897–1901.
- Wolowiec D, Berger F, Ffrench P, Bryon PA, Ffrench M (1999) CDK1 and cyclin A expression is linked to cell proliferation and associated with prognosis in non-Hodgkin's lymphomas. *Leuk Lymphoma* 35: 147–157.
- Paterlini P, Suberville AM, Zindy F, Melle J, Sonnier M, et al. (1993) Cyclin A expression in human hematological malignancies: a new marker of cell proliferation. *Cancer Res* 53: 235–238.
- Liao C, Li SQ, Wang X, Muhlrad S, Bjartell A, et al. (1993) Elevated levels and distinct patterns of expression of A-type cyclins and their associated cyclin-dependent kinases in male germ cell tumors. *Int J Cancer* 108: 654–664.
- Malumbres M, Pevarello P, Barbacid M, Bischoff JR (2008) CDK inhibitors in cancer therapy: what is next? *Trends Pharmacol Sci* 29: 16–21.
- Ortega S, Prieto I, Odajima J, Martin A, Dubus P, et al. (2003) Cyclin-dependent kinase 2 is essential for meiosis but not for mitotic cell division in mice. *Nat Genet* 35: 25–31.
- Murphy M, Stinnakre MG, Senamaud-Beaufort C, Winston NJ, Sweeney C, et al. (1997) Delayed early embryonic lethality following disruption of the murine cyclin A2 gene. *Nat Genet* 15: 83–86.
- Chen W, Lee J, Cho SY, Fine HA (2004) Proteasome-mediated destruction of the cyclin a/cyclin-dependent kinase 2 complex suppresses tumor cell growth in vitro and in vivo. *Cancer Res* 64: 3949–3957.
- Wang X, Ren J, Qu X (2008) Targeted RNA interference of cyclin A2 mediated by functionalized single-walled carbon nanotubes induces proliferation arrest and apoptosis in chronic myelogenous leukemia K562 cells. *ChemMedChem* 3: 940–945.
- Czyz M, Szulawska A, Bednarek AK, Duchler M (2005) Effects of anthracycline derivatives on human leukemia K562 cell growth and differentiation. *Biochem Pharmacol* 70: 1431–1442.
- Zuryn A, Grzanka A, Stepien A, Grzanka D, Debski R, et al. (2007) Expression of cyclin A in human leukemia cell line HL-60 following treatment with doxorubicin and etoposide: the potential involvement of cyclin A in apoptosis. *Oncol Rep* 17: 1013–1019.
- Grzanka A, Zuryn A, Styczyński J, Grzanka AA, Wisniewska H (2005) The effect of doxorubicin on the expression of cyclin A in K-562 leukemia cell line. *Neoplasma* 52: 489–493.
- Hoang AT, Cohen KJ, Barrett JF, Bergstrom DA, Dang CV (1994) Participation of cyclin A in Myc-induced apoptosis. *Proc Natl Acad Sci USA* 91: 6875–6879.
- Meikrantz W, Schlegel R (1996) Suppression of apoptosis by dominant negative mutants of cyclin-dependent protein kinases. *J Biol Chem* 271: 10205–10209.
- Meikrantz W, Gisselbrecht S, Tam SW, Schlegel R (1994) Activation of cyclin A-dependent protein kinases during apoptosis. *Proc Natl Acad Sci USA* 91: 3754–3758.
- Hirumura K, Pippin JW, Blonski MJ, Roberts JM, Shankland SJ (2002) The subcellular localization of cyclin dependent kinase 2 determines the fate of mesangial cells: role in apoptosis and proliferation. *Oncogene* 21: 1750–1758.
- Wang S, Hasham MG, Isordia-Salas I, Tsygankov AY, Colman RW, et al. (2003) Upregulation of Cdc2 and cyclin A during apoptosis of endothelial cells induced by cleaved high-molecular-weight kininogen. *Am J Physiol Heart Circ Physiol* 284: H1917–1923.
- Horiguchi-Yamada J, Yamada H, Nakada S, Ochi K, Nemoto T (1994) Changes of G1 cyclins, cdk2, and cyclin A during the differentiation of HL60 cells induced by TPA. *Mol Cell Biochem* 132: 31–37.
- Kiyokawa H, Richon VM, Rifkind RA, Marks PA (1994) Suppression of cyclin-dependent kinase 4 during induced differentiation of erythroleukemia cells. *Mol Cell Biol* 14: 7195–7203.
- Ito Y, Takeda T, Sakon M, Monden M, Tsujimoto M, et al. (2000) Expression and prognostic role of cyclin-dependent kinase 1 (cdc2) in hepatocellular carcinoma. *Oncology* 59: 68–74.
- Yoshizumi M, Lee WS, Hsieh CM, Tsai JC, Li J, et al. (1995) Disappearance of cyclin A correlates with permanent withdrawal of cardiomyocytes from the cell cycle in human and rat hearts. *J Clin Invest* 95: 2275–2280.
- Rieber M, Rieber MS (1994) Cyclin-dependent kinase 2 and cyclin A interaction with E2F are targets for tyrosine induction of B16 melanoma terminal differentiation. *Cell Growth Differ* 5: 1339–1346.
- Liu Z, Davis C, Cai W, He L, Chen X, et al. (2008) Circulation and long-term fate of functionalized, biocompatible single-walled carbon nanotubes in mice probed by Raman spectroscopy. *Proc Natl Acad Sci USA* 105: 1410–1415.

Found at: doi:10.1371/journal.pone.0006665.s007 (1.96 MB TIF)

Figure S8 Representative microscopy images of the NBT reduction assay of K562 cells after various treatments. Cells were transfected with cyclin A2 siRNA or not two hours prior to the addition of 0.4 μM DOX. Ninety six hours later, NBT dye reduction was used to qualitatively monitor monocyte-macrophage differentiation. Cells were viewed and counted using an Olympus BX-51 optical system microscope (Tokyo, Japan) at 200× magnification. Two independent tests were performed. Pictures were taken with an Olympus digital camera.
Found at: doi:10.1371/journal.pone.0006665.s008 (0.34 MB TIF)

Acknowledgments

We thank Yong Chen (College of Life Science, Jilin University) and Professor Yongchen Zheng (Central Laboratory of the 2nd Hospital, Jilin University) for their technical assistance.

Author Contributions

Conceived and designed the experiments: JR XQ. Performed the experiments: XW. Analyzed the data: XW YS JR. Contributed reagents/materials/analysis tools: YS. Wrote the paper: XW JR XQ.

35. Liu Z, Winters M, Holodniy M, Dai H (2007) siRNA delivery into human T cells and primary cells with carbon-nanotube transporters. *Angew Chem Int Ed Engl* 46: 2023–2037.
36. Kam NW, Liu Z, Dai H (2006) Carbon nanotubes as intracellular transporters for proteins and DNA: an investigation of the uptake mechanism and pathway. *Angew Chem Int Ed Engl* 45: 577–581.
37. Li X, Peng Y, Ren J, Qu X (2006) Carbon nanotubes selective destabilization of duplex and triplex DNA and inducing B-A transition in solution. *Nucleic Acids Res* 34: 3670–3676.
38. Li X, Peng Y, Ren J, Qu X (2006) Carboxyl-modified single-walled carbon nanotubes selectively induce human telomeric i-motif formation. *Proc Natl Acad Sci USA* 103: 19658–19663.
39. Peng Y, Li X, Ren J, Qu X (2007) Single-walled carbon nanotubes binding to human telomeric i-motif DNA: significant acceleration of S1 nuclease cleavage rate. *Chem Commun (Camb)* 48: 5176–5178.
40. Zhao C, Peng Y, Song Y, Ren J, Qu X (2008) Self-assembly of single-stranded RNA on carbon nanotube: polyadenylic acid to form a duplex structure. *Small* 4: 656–661.
41. Zhao C, Ren J, Qu X (2008) Single-Walled Carbon Nanotubes Binding to Human Telomeric i-Motif DNA Under Molecular-Crowding Conditions: More Water Molecules Released. *Chemistry* 14: 5435–5439.
42. Gewirtz DA (1999) A critical evaluation of the mechanisms of action proposed for the antitumor effects of the anthracycline antibiotics adriamycin and daunorubicin. *Biochem Pharmacol* 57: 727–741.
43. Minotti G, Menna P, Salvatorelli E, Cairo G, Gianni L (2004) Anthracyclines: molecular advances and pharmacologic developments in antitumor activity and cardiotoxicity. *Pharmacol Rev* 56: 185–229.
44. Karlsson M, Jungnelius U, Aamdal S, Boeryd B, Carstensen J, et al. (1996) Correlation of DNA ploidy and S-phase fraction with chemotherapeutic response and survival in a randomized study of disseminated malignant melanoma. *Int J Cancer* 65: 1–5.
45. Stål O, Skoog L, Rutqvist LE, Carstensen JM, Wingren S, et al. (1994) S-phase fraction and survival benefit from adjuvant chemotherapy or radiotherapy of breast cancer. *Br J Cancer* 70: 1258–1262.
46. Kawashima R, Haisa M, Kimura M, Takaoka M, Shirakawa Y, et al. (2004) Cyclin A correlates with the sensitivity of human cancer cells to cytotoxic effects of 5-FU. *Int J Oncol* 24: 273–278.
47. Huuhtanen RL, Wiklund TA, Blomqvist CP, Bohling TO, Virolainen MJ, et al. (1999) A high proliferation rate measured by cyclin A predicts a favourable chemotherapy response in soft tissue sarcoma patients. *Br J Cancer* 81: 1017–1021.
48. Rodriguez-Pinilla M, Rodriguez-Peralto JL, Hitt R, Sanchez JJ, Ballestin C, et al. (2004) Cyclin A as a predictive factor for chemotherapy response in advanced head and neck cancer. *Clin Cancer Res* 10: 8486–8492.
49. Yam CH, Fung TK, Poon RY (2002) Cyclin A in cell cycle control and cancer. *Cell Mol Life Sci* 59: 1317–1326.
50. Yong PR (1989) An improved method for the detection of peroxidase-conjugated antibodies on immunoblots. *J Virol Methods* 24: 227–236.